

Dynamics of rotation of a particle under the effect of a turbulent flow

Supervised by Enrico Calzavarini, assistant professor

Daphné Bouilliez, Marine Gilbert and Jeanne Lepêtre

3rd year of Bachelor's degree in Mechanical Sciences and Engineering

2018-2019

Acknowledgments

We would like to thank especially our tutor, Mister Enrico Calzavarini, for having accompanied us throughout this project. His involvement, dedication and guidance have been invaluable. He knew how to make himself available, to listen and did not count his time to pass on his knowledge.

Thank you as well to Madame Stéphanie Mathez-Bagot for having guided and advised us during the redaction of our report. She provided us with the necessary techniques to prepare our oral presentation. Her attentive ear has allowed us to improve the quality of our work.

Finally, we thank Mister Emmanuel Leriche, the Director of the Department of Mechanics, for the opportunity he offers us to conduct a research project with a teacher-researcher.

Abstract

The aim of our project was to study the dynamics of rotation of a particle under the effect of a turbulent flow. The peculiarity of a turbulent flow is that it is chaotic, unpredictable. We were interested in a particular type of turbulence, the convective turbulence.

Using computer programs, we performed simulations of two flows. One was laminar, the other was turbulent, and these two flows differed simply in their Rayleigh number. Indeed, the laminar flow had a low Rayleigh number, of the order of 10^5 , and the turbulent flow had a high Rayleigh number, of the order of 10^9 . The Rayleigh number allows to determine the stability of a flow and it depends on the temperature difference between two heat sources. Thus, the higher the difference is the greater the Rayleigh number is. Finally, the higher this number is, the more the system is unstable.

We looked if we could observe a preferential alignment for particles within these two types of flows. For that, we were interested in particles having a different aspect ratio. This aspect ratio, noted α , corresponds to the ratio between the length and the diameter of the particle. Thus, we studied the evolution of particles within a turbulent flow for three aspect ratios different: $\alpha=1$ (sphere), $\alpha=2.8$ and $\alpha=100$ (elongated particles called fibers).

Then, we performed a statistical analysis of the data, recovered thanks to computer programs, of particle trajectory to find out whether or not they had a preferential alignment. For this, we introduced two physical quantities: M and \dot{p}^2 . M corresponds to the nematic order parameter and \dot{p}^2 corresponds to the squared rotation rate.

The study of these two parameters allowed us to notice that, for both types of flows, the elongated particles tend to align horizontally with the walls. It is the same for particles with an aspect ratio of 2.8. However, we have observed that the spherical particles as well as all the particles located in the center of the flow do not have a preferential alignment. Indeed, they are oriented randomly. Finally, we have noticed that the alignment of the particles is related to the turbulence, more or less low, of the flow.

Summary

| | |
|---|-----------|
| Acknowledgments | 3 |
| Abstract | 4 |
| Introduction | 6 |
| 1. Motivations | 7 |
| 1.1. Economic | 7 |
| 1.2. Environment | 7 |
| 1.3. Industrial production | 8 |
| 1.4. Marine biology | 9 |
| 2. Problem presentation | 10 |
| 2.1. System presentation | 10 |
| 2.1.1. Atmospheric convection | 10 |
| 2.1.2. A simplified model | 11 |
| 2.2. Presentation of the equations governing the system | 11 |
| 2.2.1. Eulerian component of the model | 11 |
| 2.2.2. Lagrangian component of the model | 13 |
| 2.3. Visualization of the flow | 14 |
| 2.3.1. Low | 14 |
| 2.3.2. High | 16 |
| 3. Results | 18 |
| 3.1. Derivation of Jeffery's equation in two-dimensions | 18 |
| 3.2. Statistical analysis | 20 |
| 3.2.1. Orientation | 20 |
| 3.2.2. Rotation rate | 27 |
| Conclusion | 35 |
| Bibliography | 36 |

Introduction

Dynamics of rotation of a particle under the effect of a turbulent flow

There are 1500 active volcanoes on Earth. About sixty of these volcanoes erupt each year. A multitude of dust particles is then ejected. These particles are subsequently entrained in a turbulent flow. Then they rotate in a chaotic, unpredictable way. Researchers are trying to understand this phenomenon and analyze it. However, every particles ejected by volcanoes do not have the same aspect ratio. That is why, we will study this phenomenon for more or less elongated particles, called fibers.

The objective of our project is to analyze the rotation dynamics of a particle in a specific type of turbulence, the convective turbulence. To do this, we will perform a statistical analysis of elongated fiber trajectory data. We will then be able to observe whether or not, there is a preferential alignment of the particles.

This study leads us to ask the following question: « how do the orientation and the rotation speed of a particle in a turbulent flow vary? ».

In order to answer this question, we will, at first, detail the motives of this research. In fact, turbulent flows are encountered in many fields such as the environment or industrial production for example. The study of the evolution of a preferential alignment of the particles in this flow would enable us to understand certain phenomena.

Then, we will be interested in some equations like the Navier-Stokes' equation, the conservation of the mass, the conservation of the energy or the Jeffery's equation. These equations will form systems of equations that will be solved by a first computer program that will send back data about the flow. With these data, we can visualize two types of flow that differ in their level of turbulence.

Finally, the data collected by the previous program will be read in two other computer programs. The latter will send us text files giving us information about each particle, such as their orientation or their rotation rate. Thus, we will be able to perform a statistical analysis of these two last physical quantities by tracing their evolutions according to the height at the wall of the particles.

1. Motivations

1.1. Economic

In 2010, the Eyjafjallajökull volcano erupted. A volcanic plume, composed of water vapor, volcanic gas and ashes was formed and rose to almost 4300m altitude. This cloud was extremely dangerous for airplanes in flight. Indeed, smoke from volcanoes can cause serious damage to aircraft engines by smothering them through metal particles it contains. This smoke can also distort the probes located on the cabin of the plane, while these are essential to the smooth running of a flight because they can collect information on the flight. That is why many European countries then closed their airspace. Thus, Europe was literally paralyzed; 28 countries had to close their airspace or restrict flights. In addition, it is estimated that nearly 1.5 billion euros to 2.5 billion euros were lost because of this eruption. This loss of money concerned airlines as well as travelers and tour operators.

We wonder if this paralysis of Europe, but also, if the loss of money, could have been limited if we had been able to predict the behavior of the particles inside the volcanic plume. If that was the case, some countries that had closed their airspaces as a precaution could have been able to authorize aircraft movement if we had known exactly how the smoke particles would evolve.

But economic motivation is not the only reason that drives us to study this subject. Another motivation concerns us all, and should be a preoccupation of everyone: the environment.

1.2. Environment

In the air we breathe there are particles called $pm_{2,5}$ and pm_{10} . These two types of particles are fine particles in suspension which differ in their diameters. In fact, pm_{10} are particles whose diameter is between 2,5 and 10 micrometers, whereas $pm_{2,5}$ are particles whose diameter is less than 2,5 micrometers. It should be known that half of these particles in the air are emitted by vehicles and 90% of the particles emitted by vehicles are emitted by diesel vehicles.

The emission of these particles is something which is very worrying. Indeed, these particles are very harmful for our health. When we breathe, we breathe these particles. They will then settle in our lungs in depth, while having the ability to transport, on their surfaces, carcinogenic compounds.

What happens to these particles once they are released into the air? This is a question we could answer if we better understand the evolution of particles in a turbulent flow.

Our project could then lead to environmental and health developments, but it could also provide information to understand in a better way the industrial production sector.

1.3. Industrial production

The paper may be composed of one or more layers of cellulose fibers. However, it is important to note that the properties of the paper will change depending on the alignment of these cellulose fibers. In paper-making, it is preferable that the cellulose fibers are aligned with each other, i.e. they are all parallel. This will allow the paper to be torn for example. Currently, fiber alignment for paper production can be controlled by convergents as well as scrolls.

The paper is not the only motivation we have to study particles placed in a turbulent flow because there is also the production of plastic to make bumper cars for example. In fact, these bumpers are made of glass fibers which, depending on their alignment, will allow the bumpers to be more or less resistant during a shock on them.

By understanding how particles behave in a turbulent flow, we could then improve the properties of materials manufactured in the industrial sector.

However, there are still other sectors for which it would be very interesting to understand the movement of particles, such as marine biology.

1.4. Marine biology

In the oceans, there are what are called plankton. Plankton are microscopic organisms, very often unicellular and living in fresh or salt water. They are therefore living beings who live in suspension and apparently passively because they are unable to fight against the marine current. We will focus on one type of plankton in particular: phytoplankton. Phytoplankton is the plant plankton, that is all living plant organisms suspended in water and it converts carbon dioxide into oxygen. However, phytoplankton can not swim. Then, we imagine that this elongated alga has just adopted this particular form to allow it to catch food or to reproduce, otherwise this living being would have disappeared.

We can therefore think that it is thanks to the turbulence of the oceans and to the movement of particles in this turbulent flow that biology has been preserved, and it would be extremely interesting to understand how this was possible.

Through the study of all these motivations, we have been able to understand the interest and purpose of our integrative project. This allowed us to better visualize the problem as well as the objectives to be achieved. After understanding all this, we continued the study of this project trying to understand the evolution of particles in a turbulent flow.

2. Problem presentation

In order to understand the system, it is necessary to know how it works and especially thanks to which equations.

2.1. System presentation

2.1.1. Atmospheric convection

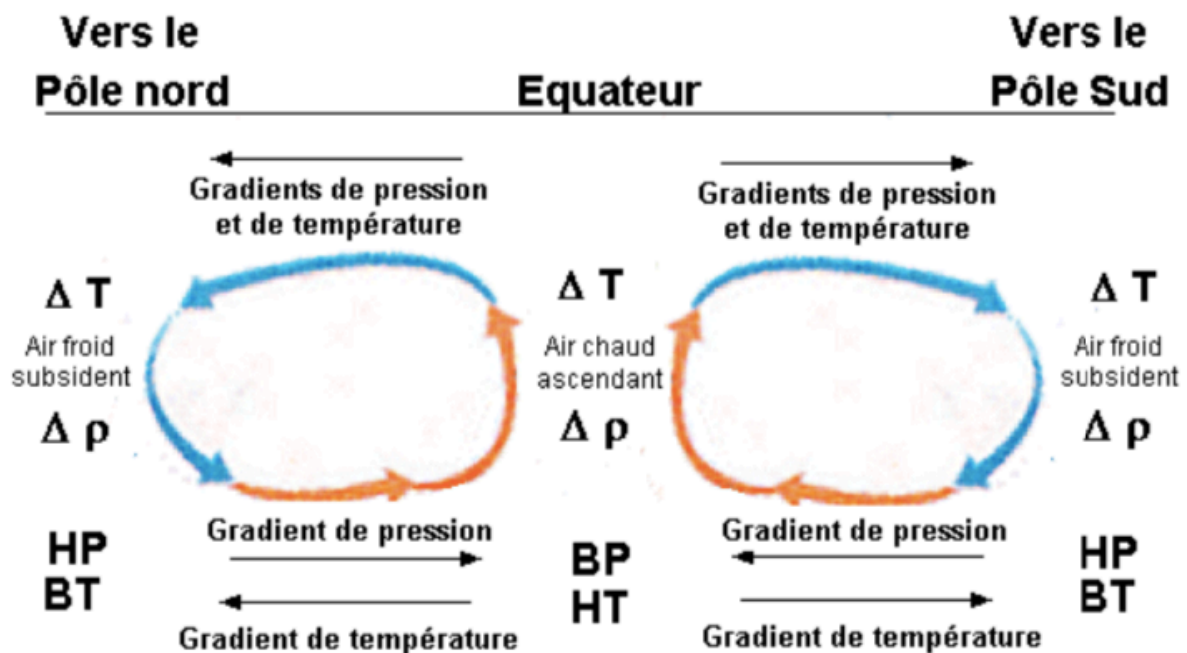


Figure 1 – drawing schematizing the atmospheric convection © Dionysos, IUFM de Bretagne

On our planet, the sun warms the surface of the Earth and the Earth itself warms the air. However, we know that solar energy is unequally distributed on the surface of the Earth. Differences of temperature will therefore cause instability of the air.

So, at the equator, where the Earth is the closest to the sun, the temperature is higher. The warm air, less dense, will therefore undergo an Archimedes push up. This air will rise and then cool down towards the poles. At the poles, the colder air, and therefore more dense, will go down and go towards the equator while warming up. It's atmospheric convection.

However, this type of convection is very widespread. That is why we will use a simplified model of atmospheric convection to be able to create our system.

2.1.2. A simplified model

We want to study the movement of small particles in a turbulent flow. For that, we will use a simplified and idealized model of the atmosphere by placing particles of different sizes between a hot plate and a cold plate. Thus, a turbulent convective flow will be created, like the one of atmospheric convection.

The system considered will be, therefore, a two-dimensional system, of rectangular shape, heated from below and cooled from above. The hydrodynamic instability will lead to convective fluid motion.

On the Earth, this system whose turbulence is linked to convection, is omnipresent. Indeed, we can meet him in the oceans, as in the atmosphere for example. Thanks to the study of the system and the motion of the particles within it, we may be able to better understand how non-spherical particles evolve in a turbulent flow, and thus understand some phenomena cited in the motivations.

In order to create this two-dimensional convective system, we need to understand some equations and their interests.

2.2. Presentation of the equations governing the system

2.2.1. Eulerian component of the model

The Eulerian component corresponds to the part involving fields. These fields correspond to physical quantities that depend on both position and time. In our system, we will focus on velocity and temperature fields.

In this first part, we will mainly use the Boussinesq system, that is to say an extension of the Navier-Stokes equations made to include relatively weak thermal forcings. The Boussinesq system is a system that works in the case of incompressible flow. It is very useful in many developments, and more particularly for phenomena with a difference of temperature. Therefore this system is very well adapted to the convection problem that we are studying. It was introduced in 1877 by Joseph Boussinesq, professor of

mechanics at the University of Lille (Boussinesq, J. 1903 Theorie analytique de la chaleur, Vol. 2 . Paris: Gauthier-Villars).

Boussinesq's system uses equations capable of describing the motion of an incompressible fluid: the the conservation equation of momentum, the conservation equation of mass, and the energy equation. Thus, the Boussinesq system reads:

$$\left\{ \begin{array}{l} \frac{D\vec{u}}{Dt} = -\frac{\vec{\nabla}P}{\rho_0} + \nu\Delta\vec{u} + \beta g(T - T_0)\vec{z} \quad \text{conservation of momentum} \\ \vec{\nabla} \cdot \vec{u} = 0 \quad \text{conservation of the mass} \\ \frac{DT}{\partial t} = k\Delta T \quad \text{conservation of the energy} \end{array} \right.$$

with ν the kinematic viscosity, β the coefficient of thermal expansion, g the gravitational acceleration and T_0 a reference temperature (e.g. the mean between the bottom and top boundary temperatures).

The software used by our tutor (<https://github.com/ecalzavarini/ch4-project>) will solve this system of three equations to collect data about the flow and particles. Thus we will be able to use the data to study the parameters that interest us.

Let us remark that the Rayleigh-Benard system is a nonlinear system that allows to study convection, although in an idealized way. This system introduces a dimensionless number, the Rayleigh number, noted Ra. This number makes it possible to determine the stability of the system.

$$Ra = \frac{\beta g h^3 (T_1 - T_0)}{\nu k}$$

where k is the thermal diffusivity and h the distance between the two heat sources

We can see that the Rayleigh number is proportional to the temperature gradient. Thus, the stability of our system depends on this number. Indeed, more the temperature of the lower plate (hot plate) will be elevated compared to the upper plate (cold plate), more the Rayleigh number will be high. Therefore, the higher the Rayleigh number of our system is, the more unstable it will be. There is a critical threshold for the Rayleigh number. When it

is exceeded, the system becomes unstable and it is then that the convection is observed. This threshold corresponds to a Rayleigh number equal to 1708.

2.2.2. Lagrangian component of the model

The Lagrangian component of the model corresponds to the part where we study directly the particles which we consider as material points.

We will study the quantity \vec{r} , that is to say the vector position of the particle. This is not a field because it depends only on time, not time and position. Likewise, we will be interested in the quantity \vec{p} which corresponds to the vector unit of orientation of the particle. So, \vec{r} and \vec{p} are two functions that form the following system:

$$\left\{ \begin{array}{ll} \vec{r}(t) = \vec{u}(r, t) & \textit{particle's trajectory equation} \\ \dot{\vec{p}}(t) = \Omega \vec{p} + \frac{\alpha^2 - 1}{\alpha^2 + 1} (S \vec{p} - (\vec{p}^T S \vec{p}) \vec{p}) & \textit{Jeffery's equation} \end{array} \right.$$

Thus, this system of equations describes both the motion of the particles (specifically the motion of their center of mass) and the orientation of the particles in a turbulent flow. In the third part, we will demonstrate Jeffery's equation. This equation gives us the dynamics of the vector orientation of an ellipsoidal axially symmetric particle with negligible inertia in a linear spatial flow. It was introduced by George Barker Jeffery, physicist mathematician, in 1922 (Jeffery, G. B. (1922). "The Motion of Ellipsoidal Particles Immersed in a Viscous Fluid". Proceedings of the Royal Society A: Mathematical, Physical and Engineering Sciences. 102 (715): 161.). Indeed, he published an article describing the movement of particles in a viscous fluid and describing what is now called the Jeffery equation. This equation, quite complex, gives us the speed of rotation and the orientation of the particles in a turbulent flow.

Thanks to the Eulerian component, we were able to obtain the data of a turbulent flow. Then, using the Lagrangian component, we were able to obtain information about the particles as their positions or orientations.

Thus we were able to visualize the movement of particles in a turbulent flow by making a film by juxtaposing images of the flow at different times.

2.3. Visualization of the flow

We have performed two simulations to obtain two flow visualizations. These two simulations are very different from each other since the parameters differ from one simulation to another, notably the number of Rayleigh. Indeed, in the first simulation which we will call « low », the Rayleigh number is much lower than in the second, « high », in which the Rayleigh number is high. Thus, the « low » simulation is laminar while the « high » simulation is in a turbulent state. In this last one, the Rayleigh number is greater than 1700, that is to say it is upper than the threshold from which the system becomes convective.

These visualizations of the flows were obtained using a computer program (annex n°1). A basic program was provided by our tutor, we had to modify it to adapt it to the data also provided by our tutor. This program has read this data. Then, it makes a graph that indicates the position of the particles in the flow, between the two walls.

2.3.1. Low

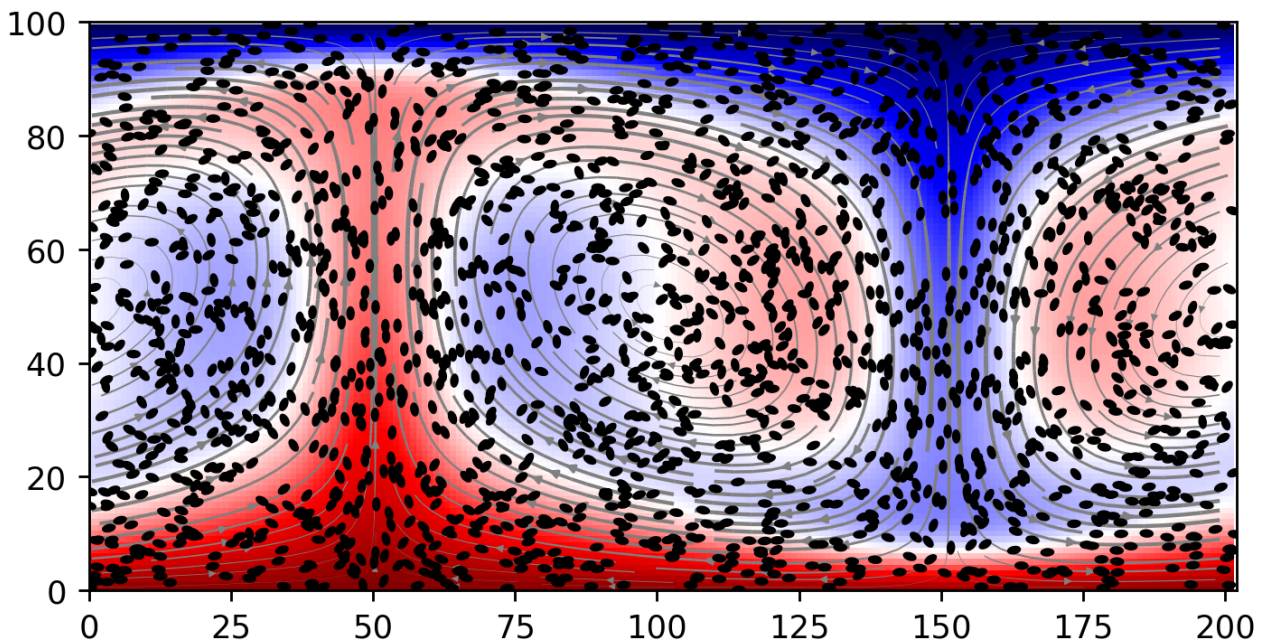


Figure 2 — visualisation of the « low » flow, the flow with the low Rayleigh number ($Ra \sim 10^5$) © Bouilliez, Gilbert, Lepêtre

Figure n°2 represents a visualization of the « low » flow, flow with the low Rayleigh number. The particles are here colored in black. The red areas indicate the areas where the temperature is high, while the areas where the temperature is low are shown in blue. We notice that at the bottom wall, that is to say for the coordinate $y=0$, the graph represents the flow by the red color, which well corresponds to the fact that the bottom plate is the hottest. Thus, we notice that at the top wall, $y=100$, the graph is represented by the blue color, which corresponds to the coldest plate.

Moreover, we can notice that when we move away from the walls ($y=0$ and $y=100$), vortices are formed. Inside these vortices, the temperature can be high, or low. This illustrates the laminar convective flow. We notice that the hot material will go up to the cold plate, then in contact with this wall, the material will go down. This material, in contact with the cold wall, will lose heat. Therefore, we can observe an attenuation of the red color in the vortices of the graph. The same phenomenon is noticeable for the cold material. Indeed, it will go down to the hot plate and thus increase its temperature.

Finally, we can notice that at the lower and upper walls ($y=0$ and $y=100$), the particles seem aligned horizontally. The particles located inside the flow, and therefore far from the walls, seem to have much more random alignments. We will put in place parameters, in the third part, which we will then study and will allow us to confirm, or not, this conjecture.

Let's now look at the visualization of the "high" flow, with the high Rayleigh number.

2.3.2. High

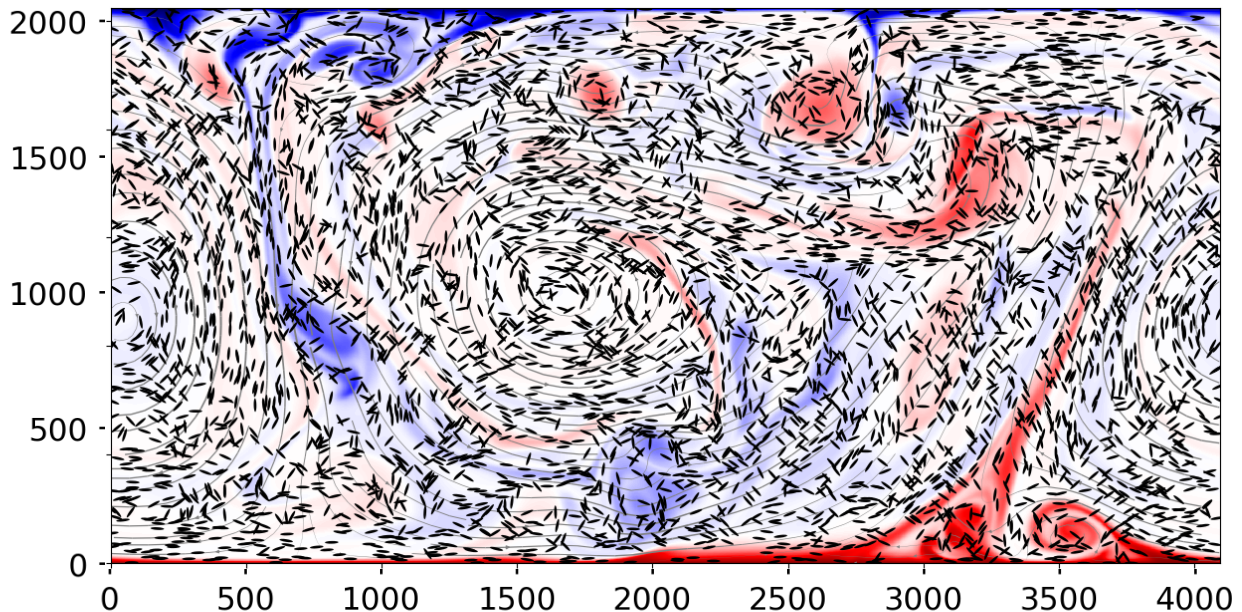


Figure 3 — visualisation of the « high » flow, the flow with the high Rayleigh number ($Ra \sim 10^9$) © Calzavarini

Figure n°3 represents a visualization of the « high » flow, flow with a high Rayleigh number. As for the « low » flow, the zones colored in red represent the areas where the temperature is higher than the mean and the areas in blue those where the temperature is low.

We can notice that the hot plate is the lower plate and the upper plate is the cold plate. We also note the presence of small vortices where the temperature is either high or low inside the flow. In these ones, the particles have different orientations and they have no preferential alignment.

Finally, we notice that the particles tend to align horizontally with the walls. Indeed, the particles are horizontal at the walls ($y=0$ and $y=2000$).

The two visualizations, « low » and « high », allow us to notice that there seems to be a preferential alignment of the particles at the level of the walls. Indeed, for these two flows, the particles appear aligned horizontally to the wall. However, in the vortices of turbulent

convective flows « low » and « high », we can not affirm if there is a preferential orientation of the particles or not.

Afterwards, we will try to study the orientation and speed of rotation of the particles to understand the evolution of these in two types of turbulent flows. For that, we will demonstrate Jeffery's equation in order to better understand where it comes from and what it allows to calculate. In addition, we will use computer programs to perform statistical analysis on two physical quantities; orientation and rotation rate.

3. Results

3.1. Derivation of Jeffery's equation in two-dimensions

We thought it was essential to understand the Jeffery equation. That's why we got familiar with its three-dimensional form, and from that, we derived its expression in a two-dimensional geometry.

The dynamics of the orientation unit vector \vec{p} of an ellipsoidal an inertialess axi-symmetric particle in a spatially linear flow is described by the following equation, Jeffery's equation:

$$\dot{\vec{p}} = \Omega \vec{p} + \lambda (S \vec{p} - (\vec{p}^T S \vec{p}) \vec{p})$$

with Ω the rate of rotation tensor, $\Omega = \frac{1}{2}(\nabla \vec{u} - (\nabla \vec{u})^T)$

with S the rate of strain tensor, $S = \frac{1}{2}(\nabla \vec{u} + (\nabla \vec{u})^T)$

with $\lambda = \frac{\alpha^2 - 1}{\alpha^2 + 1}$ where α is the aspect ration, the length over diameter $\alpha = l/d$

and $\nabla \vec{u}(\vec{x}_p, t)$ is the fluid velocity gradient tensor at the particle position \vec{x}_p which is defined as:

$$\nabla \vec{u} = \begin{pmatrix} \frac{\partial u_x}{\partial x} & \frac{\partial u_x}{\partial y} & \frac{\partial u_x}{\partial z} \\ \frac{\partial u_y}{\partial x} & \frac{\partial u_y}{\partial y} & \frac{\partial u_y}{\partial z} \\ \frac{\partial u_z}{\partial x} & \frac{\partial u_z}{\partial y} & \frac{\partial u_z}{\partial z} \end{pmatrix}$$

and $\nabla \vec{u} = \Omega + S$, where Ω is the symmetric part of the velocity gradient and S the anti antisymmetric part.

In two-dimension, the expression of the orientation vector, the vector \vec{p} , is simplified by:

$$\vec{p} = \begin{pmatrix} p_x \\ p_y \end{pmatrix} = \begin{pmatrix} \cos \theta \\ \sin \theta \end{pmatrix}$$

Once derived by the time, it gives:
$$\dot{\vec{p}} = \begin{pmatrix} \dot{p}_x \\ \dot{p}_y \end{pmatrix} = \begin{pmatrix} -\dot{\theta} \sin \theta \\ \dot{\theta} \cos \theta \end{pmatrix}$$

Also, in two-dimension, the Jeffery's equation can be simplified by using the following relations:

$$\Omega = \begin{pmatrix} 0 & \Omega_{12} \\ -\Omega_{12} & 0 \end{pmatrix} = \begin{pmatrix} 0 & \frac{1}{2} \left(\frac{\partial u_x}{\partial y} - \frac{\partial u_y}{\partial x} \right) \\ \frac{1}{2} \left(\frac{\partial u_y}{\partial x} - \frac{\partial u_x}{\partial y} \right) & 0 \end{pmatrix} = \begin{pmatrix} 0 & -\omega/2 \\ \omega/2 & 0 \end{pmatrix}$$

$$S = \begin{pmatrix} S_{11} & S_{12} \\ S_{12} & S_{22} \end{pmatrix} = \begin{pmatrix} \frac{\partial u_x}{\partial x} & \frac{1}{2} \left(\frac{\partial u_x}{\partial y} + \frac{\partial u_y}{\partial x} \right) \\ \frac{1}{2} \left(\frac{\partial u_y}{\partial x} + \frac{\partial u_x}{\partial y} \right) & \frac{\partial u_y}{\partial y} \end{pmatrix} = \begin{pmatrix} S_{11} & S_{12} \\ S_{12} & -S_{11} \end{pmatrix}$$

where ω is the vorticity pseudo-scalar defined as $\omega \vec{z} = \nabla \times \vec{u}$

The relation $S_{22} = -S_{11}$ is a direct consequence of the flow incompressibility, $\nabla \cdot \vec{v} = 0$.

The equation for p_x and p_y are redundant, we'll just develop the Jeffery's equation for the component x.

We project the Jeffery's equation on \vec{x} , which leads to:

$$\begin{aligned} \Rightarrow \dot{p}_x &= \Omega_{12} p_y + \lambda \left[S_{11} p_x + S_{12} p_y - (p_x S_{11} p_x + p_x S_{12} p_y + p_y S_{12} p_x + p_y S_{22} p_y) p_x \right] \\ \Leftrightarrow \dot{p}_x &= \Omega_{12} p_y + \lambda \left[S_{11} p_x + S_{12} p_y - S_{11} p_x^3 - 2S_{12} p_x^2 p_y + S_{11} p_x p_y^2 \right] \\ \Leftrightarrow \dot{p}_x &= \Omega_{12} p_y + \lambda \left[S_{11} (p_x - p_x^3 + p_x p_y^2) + S_{12} (p_y - 2p_x^2 p_y) \right] \\ \Leftrightarrow -\dot{\theta} \sin \theta &= \Omega_{12} \sin(\theta) + \lambda \left[S_{11} (\cos \theta - \cos^3 \theta + \cos \theta \sin^2 \theta) + S_{12} (\sin \theta - 2 \cos^2 \theta \sin \theta) \right] \\ \Leftrightarrow \dot{\theta} &= -\Omega_{12} - \lambda \left[S_{11} \left(\frac{1}{\tan \theta} - \frac{\cos^2 \theta}{\tan \theta} + \cos \theta \sin \theta \right) + S_{12} (1 - 2 \cos^2 \theta) \right] \end{aligned}$$

Or $\cos(2\theta) = 2 \cos^2 \theta - 1 \Leftrightarrow -\cos(2\theta) = 1 - 2 \cos^2 \theta$ whence:

$$\Leftrightarrow \dot{\theta} = -\Omega_{12} - \lambda \left[\frac{S_{11}}{\tan \theta} (1 - \cos^2 \theta + \sin^2 \theta) - S_{12} \cos(2\theta) \right]$$

Or $\cos(2\theta) = \cos^2 \theta - \sin^2 \theta \Leftrightarrow -\cos(2\theta) = -\cos^2 \theta + \sin^2 \theta$ whence:

$$\Leftrightarrow \dot{\theta} = -\Omega_{12} - \lambda \left[S_{11} \frac{1}{\tan \theta} (1 - \cos(2\theta)) - S_{12} \cos(2\theta) \right]$$

$$\text{Or } \tan \theta = \frac{1 - \cos(2\theta)}{\sin(2\theta)} \Leftrightarrow \frac{1}{\tan \theta} = \frac{\sin(2\theta)}{1 - \cos(2\theta)} \text{ whence:}$$

$$\Leftrightarrow \dot{\theta} = -\Omega_{12} - \lambda \left[S_{11} \frac{\sin(2\theta)}{1 - \cos(2\theta)} (1 - \cos(2\theta)) - S_{12} \cos(2\theta) \right]$$

$$\Leftrightarrow \dot{\theta} = \frac{1}{2}\omega - \lambda [S_{11} \sin(2\theta) - S_{12} \cos(2\theta)]$$

We notice a sign error with previous scientific articles dealing with this equation. Indeed, in the article « A. Gupta, D. Vincenzi et R. Pandit, Elliptical tracers in two-dimensionnel, homogeneous, isotropic fluid turbulence: The statistics of alignment, rotation, and nematic order, Physical Review E 89, 021001(R) (2014) », we find the following equation:

$$\dot{\theta} = \frac{1}{2}\omega + \lambda [S_{11} \sin(2\theta) - S_{12} \cos(2\theta)]$$

Our tutor has also tried to demonstrate the equation but he finds the same sign error. He informed his colleagues and authors of the previous article.

3.2. Statistical analysis

In order to understand how the orientation and the rotation rate of particles in a turbulent flow evolve, we will study two parameters: M and \dot{p}^2 . To do this, we will perform a statistical analysis of these two quantities according to their shape parameter, that is to say, their aspect ratio. In fact, we will run our computer program several times each time analyzing different aspect ratio. Thus, we can observe how the more or less elongated form of a particle affects M and \dot{p}^2 . Finally, we will also be able to notice if the distance of the particles to the wall plays a role on the parameters M and \dot{p}^2 .

We will study these parameters for two types of flow. The first, which we will call the « low » flow, is a flow in which the Rayleigh number is quite small. The second, called « high », is a flow in which the Rayleigh number is high.

3.2.1. Orientation

In this part, we will try to understand how the orientation of particles evolves in a turbulent flow. For this, we will introduce and use the parameter M , called nematic order parameter. This parameter makes it possible to quantify the spatial distribution of the

particle orientations and has already been used by « A. Gupta, D. Vicenzi, R. Pandit, Rev. E, 89, 021001 (R) (2014) » to study anisotropic particles in turbulent flows.

The parameter M is a parameter usually used in the field of nematic fluids, that is to say in the study of liquid crystals. These are materials which, depending on the orientations of the molecules that compose them, will behave either as a liquid or as a solid. The molecules that constitute these liquid crystals have an elongated shape, which makes it possible to assimilate them to the elongated particles that we will study in this project. In 2D, it suffices therefore to use the parameter M to identify the local state of a liquid crystal and this parameter is given in the form:

$$M = 2(\cos \theta)^2 - 1$$

$$\Leftrightarrow M = 2p_x^2 - 1$$

Thanks to this formula, we can obtain information on the particles of the flow. Indeed, when a particle is aligned with the horizontal, the angle θ , formed between the wall and the orientation vector \vec{p} , is zero. We know that $\cos 0 = 1$, therefore, we can say that $M = 1$ for a particle aligned horizontally. Moreover, when a particle is aligned with the vertical, the angle θ is equal to $\frac{\pi}{2}$ and $\cos(\frac{\pi}{2}) = 0$. Thus, we can say that $M = -1$ for a particle aligned vertically. Finally, when the alignment of the particle forms an angle θ such that $\theta = \frac{\pi}{4}$, this implies that $M = 0$. The following diagram (figure n°4) gives a better visualization of the influence of the alignment of a particle on the parameter M .

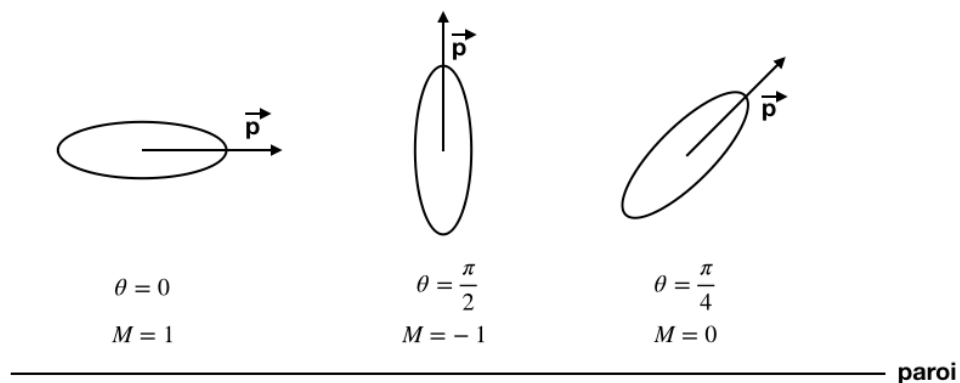


Figure 4 — influence of the alignment of a particle on the parameter M © Bouilliez, Gilbert, Lepêtre

In order to perform our statistical analysis with a computer program (annex n°2), we will perform averages on time and in space along the horizontal lines, that is the x direction, since our system only varies vertically. Thus, the average of M , denoted by $\langle M \rangle$, is a function of y , ie the vertical.

a. Flow « low »

We will start by looking at graphs of the flow called « low », the flow at low Rayleigh number. To retrieve these 3 graphs, we ran a program where only the aspect ratio changed. In fact, we have three graphs for three different aspect ratios, $\alpha=1$, $\alpha=2.8$ and $\alpha=100$, and thus different particle shapes. Here is a diagram (figure n°5) explaining the change in aspect ratio for different particle shapes.

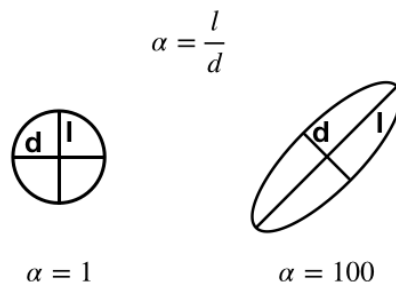


Figure 5 — aspect ratio for different particle shapes © Bouilliez, Gilbert, Lepêtre

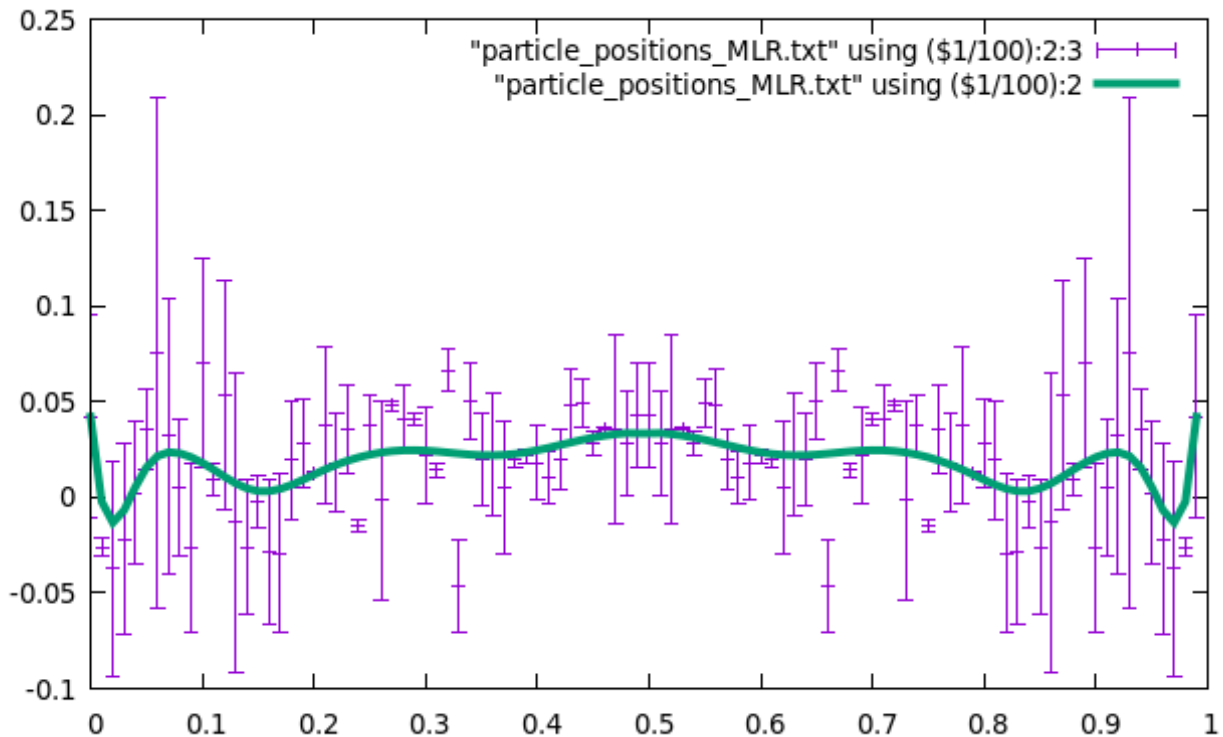


Figure 6 — the parameter M according to the height at the wall for the « low » flow and an aspect ratio $\alpha=1$ © Bouilliez, Gilbert, Lepêtre

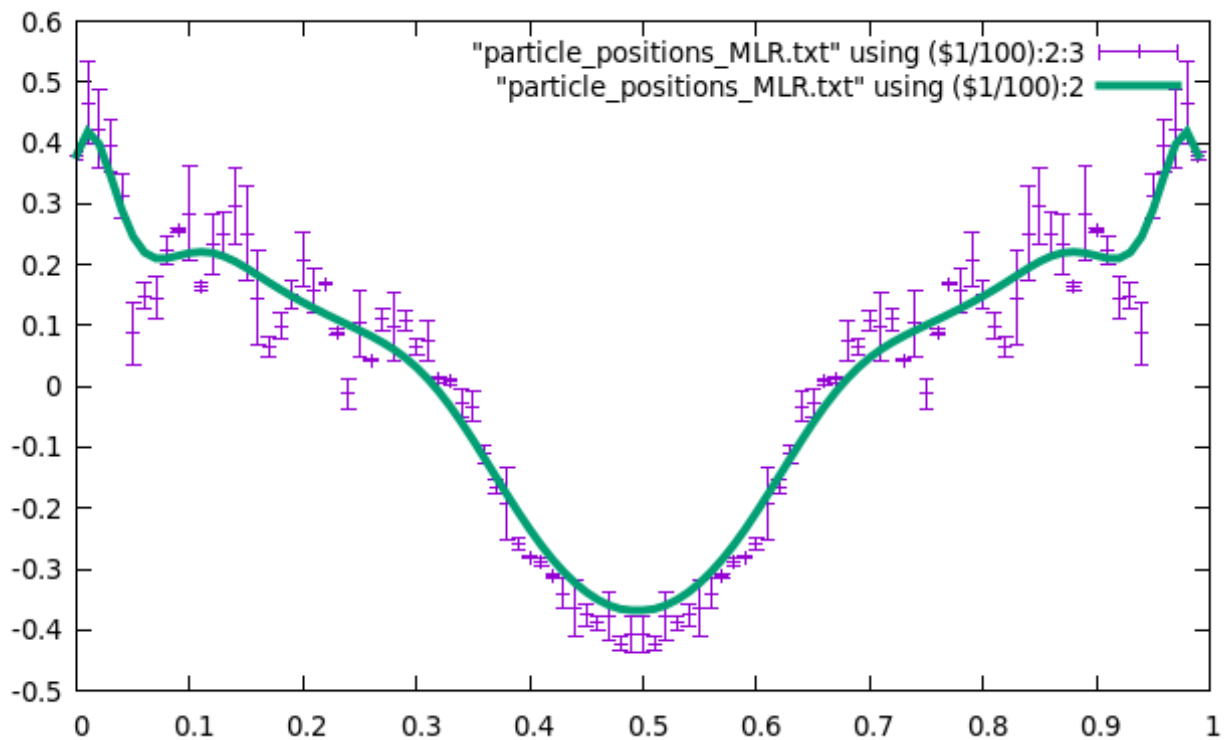


Figure 7 — the parameter M according to the height at the wall for the « low » flow and an aspect ratio $\alpha=2.8$ © Bouilliez, Gilbert, Lepêtre

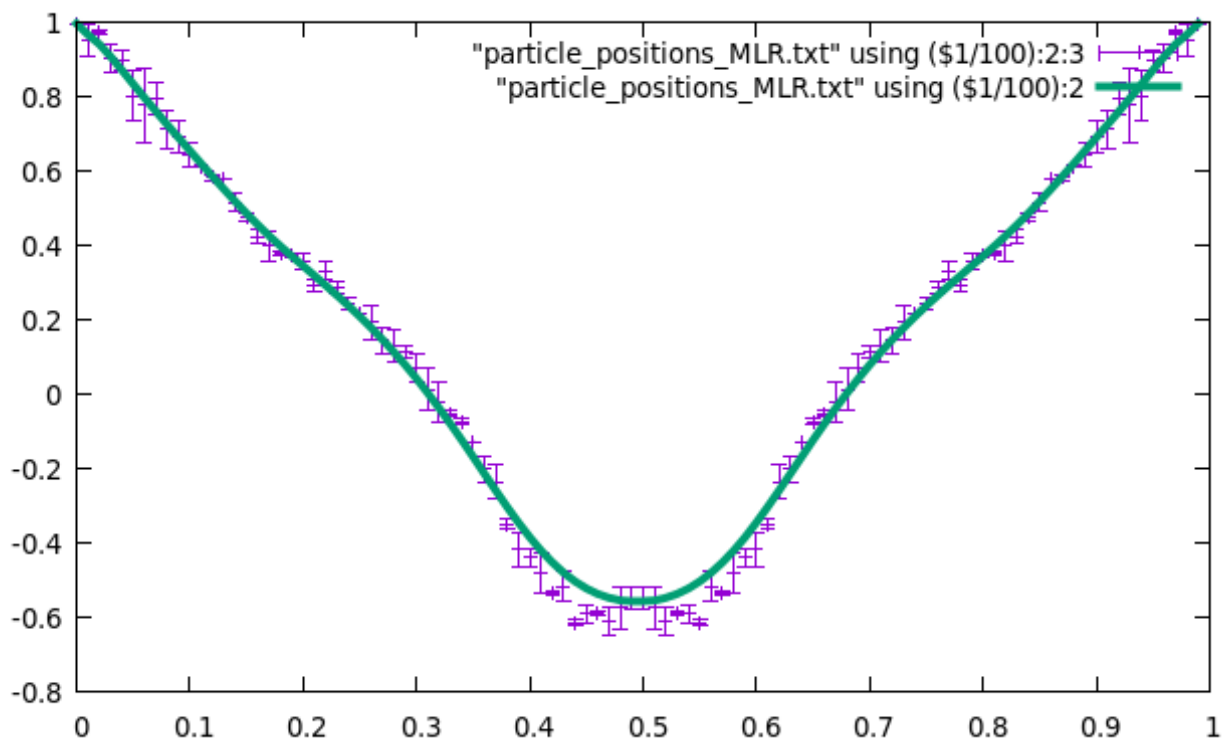


Figure 8 — the parameter M according to the height at the wall for the « low » flow and an aspect ratio $\alpha=100$ © Bouilliez, Gilbert, Lepêtre

Figure 6 relates to particles having aspect ratio $\alpha=1$. These particles therefore have a spherical shape. This figure shows the evolution of the parameter M throughout the turbulent flow. The curve plotted in green on the graph represents the average of this parameter, $\langle M \rangle$. We notice that this one oscillates around 0, one says then that it is compatible with 0. As we stated previously, when $M = 0$, two cases are possible for the orientation of the particles. In fact, either the wall and the orientation vector form an angle $\theta = \frac{\pi}{4}$, and the particles are oriented obliquely, or the particles are oriented randomly. In the latter case, that means that the particles have no preferential orientation and, when we take the average of the parameter M , the latter can vary between -1 and 1, it gives us 0. We note that, throughout the flow, the sphere-shaped particles have no preferential orientation.

Figure 7 treats particles having an aspect ratio $\alpha=2.8$. The latter is not much larger than 1 but it suffices to change the aspect ratio a little to observe a preferential alignment of the particles. In fact, on this second graph, we notice that the average of the parameter M , represented by the green curve, is not all the time equal to 0. However, as we saw previously with figure 1, if the curve of $\langle M \rangle$ is compatible with 0, that means that the particles have no preferential orientation. This allows us to say that particles with an aspect ratio $\alpha=2.8$ have preferential orientations in this turbulent flow.

Figure 8 of this « low » flow relates to particles having an aspect ratio of 100. Thus, in the latter case, we study the evolution of elongated particles, called fibers, through a turbulent flow. We notice that at the walls, that is to say in $x=0$ and $x=1$, the average of the parameter M is 1. Thus, we can say that the particles at the level of the walls have a preferential orientation because they are all aligned horizontally. In the middle of the flow, in $x=0.5$, we can observe that the curve tends to -1, which suggests to us that the particles are, at this point, vertically aligned. Finally, between both, we can see that the particles also have a preferential orientation and that they follow a very precise orientation throughout the flow.

Finally, we can notice that, on the 3 graphs, we observe a symmetry. In fact, the three curves are symmetrical with respect to the middle of the flow, that is to say $x=0.5$. This

symmetry allows us to say that we have statistics that have converged well. If we had not observed symmetry, it would have meant that we did not have enough data.

b. Flow « high »

Now, we will look at graphs for flow at high Rayleigh number, « high » flow. This flow is less regular and therefore less predictable than the previous one. We also ran the same program for the same 3 aspect ratios, $\alpha=1$, $\alpha=2,8$ and $\alpha=100$, changing the database to analyze, which is now the « high » flow one.

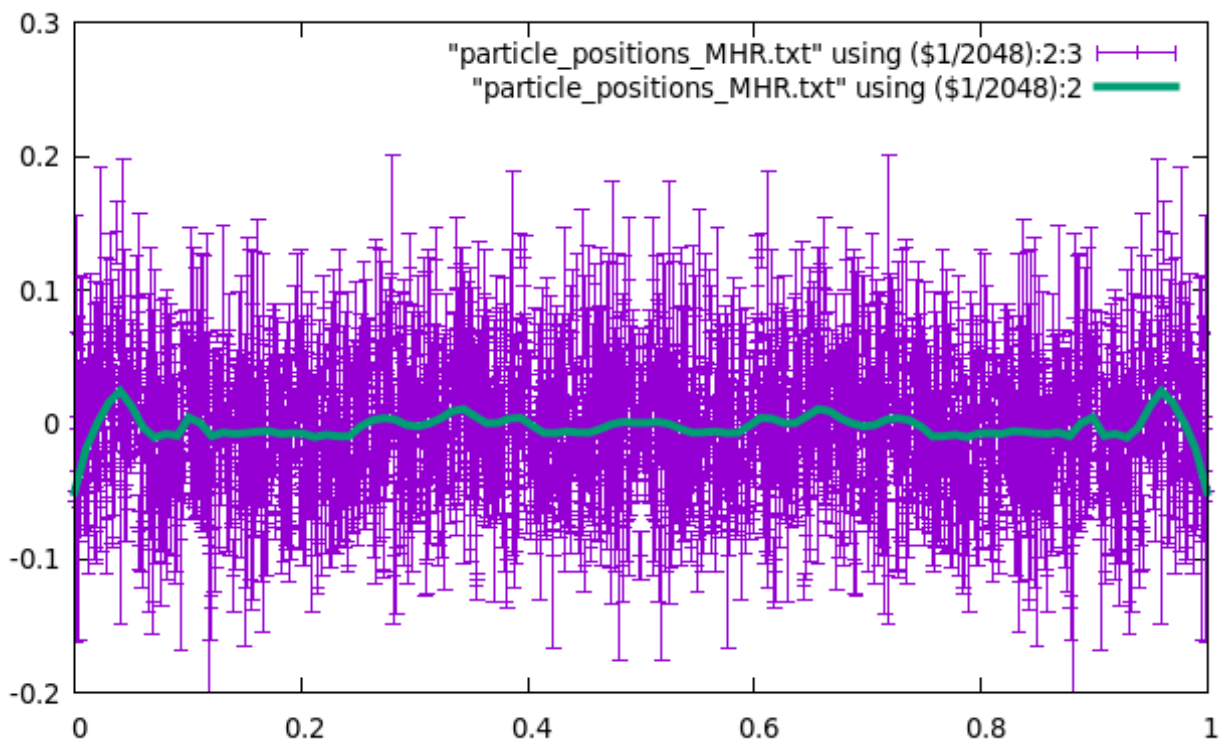


Figure 9 — the parameter M according to the height at the wall for the « high » flow and an aspect ratio $\alpha=1$ © Bouilliez, Gilbert, Lepêtre

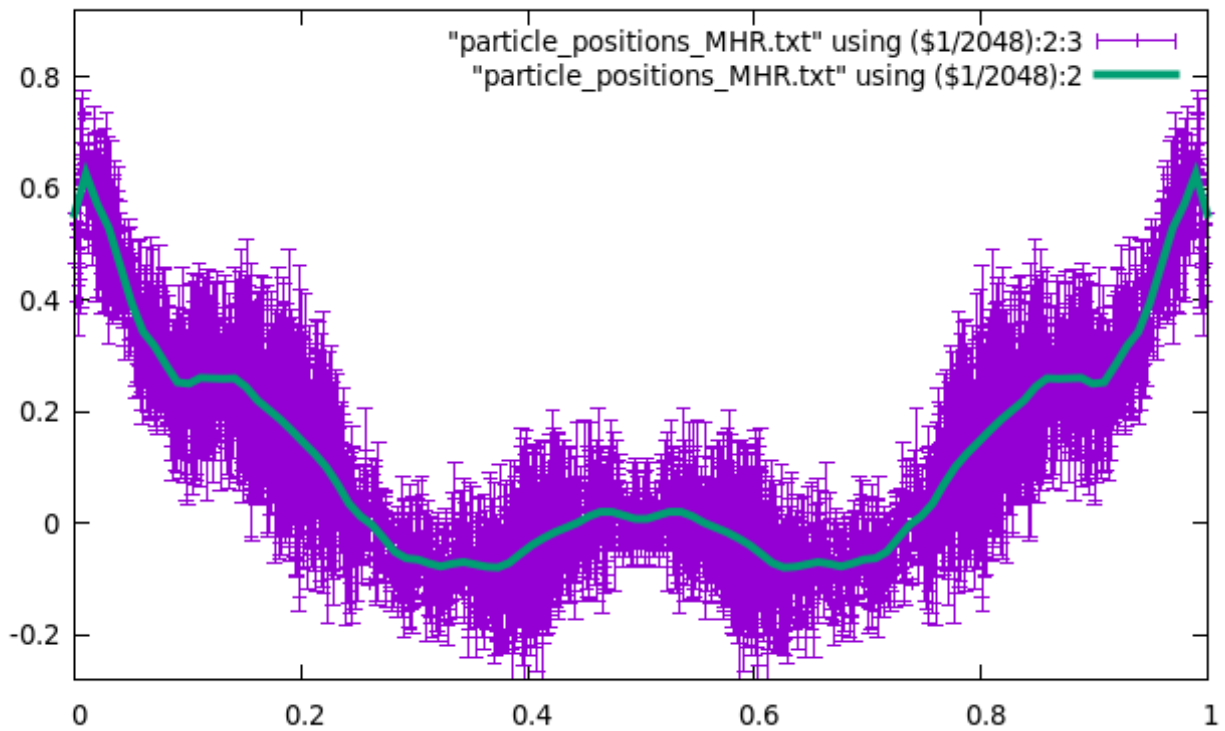


Figure 10 — the parameter M according to the height at the wall for the « high » flow and an aspect ratio $\alpha=2.8$ © Bouilliez, Gilbert, Lepêtre

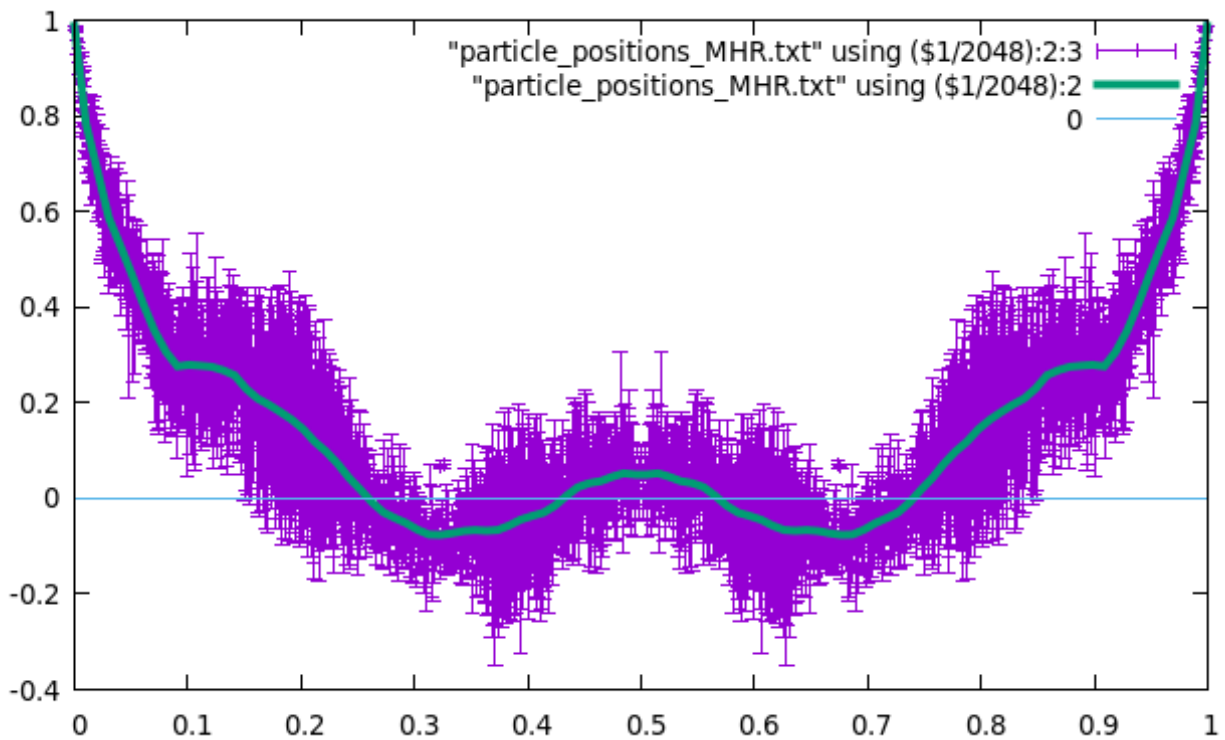


Figure 11 — the parameter M according to the height at the wall for the « high » flow and an aspect ratio $\alpha=100$ © Bouilliez, Gilbert, Lepêtre

Figure 9 shows the parameter M for the sphere-shaped particles, $\alpha=1$. We note that, as for the « low » flow, the particles have no preferential alignment. In fact, it has a random orientation because we can see that $\langle M \rangle = 0$. The spherical particles therefore have no preferential orientation in a turbulent flow, whatever it may be.

Figure 10 treats particles that have an aspect ratio $\alpha=2.8$. When the aspect ratio hardly increases, we can notice that the particles have a preferential orientation. We find that the particles tend to align horizontally with the walls, $\langle M \rangle$ approaching $y=1$ at the ends ($x=0$ and $x=1$). This preferred orientation is a little coarser than for particles of the same aspect ratio in the « low » type flow. In fact, we have much less data for this « high » flow. It would have required a larger and longer simulation.

In figure 11, these are particles with an aspect ratio of 100. They are therefore elongated particles. We can make the same observation as for the « low » flow, the particles are horizontally aligned with the walls. However, we note that when increasing the Rayleigh number, the areas where the particles have a preferential orientation are much more restricted. In fact, if we compare the two graphs $\alpha=100$, we notice that the curve decreases more sharply for the « high » flow than for the « low » flow. Finally, we notice that in the center of this flow, the curve is compatible with 0. The particles have no preferential alignment, unlike the « low » flow where the particles follow a very particular orientation between the walls.

Finally, if we look at these three graphs for the « high » flow, we also notice symmetry. This symmetry is the same as the one for the « low » flow, symmetrical with respect to $x=0.5$. Our statistics have converged and our analysis is therefore solid.

3.2.2. Rotation rate

In a second step, we decided to study the squared rotation rate, noted \dot{p}^2 , of particles placed in a turbulent convective flow. But, to simplify the equations, we have decided to work in the two-dimensional case. We can write:

$$\dot{p}^2 = \dot{p}_x^2 + \dot{p}_y^2 = \dot{\theta}^2 \sin^2 \theta + \dot{\theta}^2 \cos^2 \theta = \dot{\theta}^2 (\sin^2 \theta + \cos^2 \theta) = \dot{\theta}^2$$

Thus, we have demonstrated that, in the two-dimensional case, to study the quadratic rotation rate of a particle is like studying $\dot{\theta}^2$, that is to say to study the square of its speed

of rotation. Therefore, we will be able to use the equation of Jeffery which, as we have seen previously, makes it possible to find $\dot{\theta}$. By raising the $\dot{\theta}^2$, we will obtain \dot{p}^2 , that is to say the rotation rate.

In order to study the rotation rate of the particles and to carry out our statistical analysis, with a computer program (annex n°3), we will make averages in the x direction.

a. Flow « low »

First, we will study the variation of the rotation rate for the « low » flow, that is to say the laminar flow.

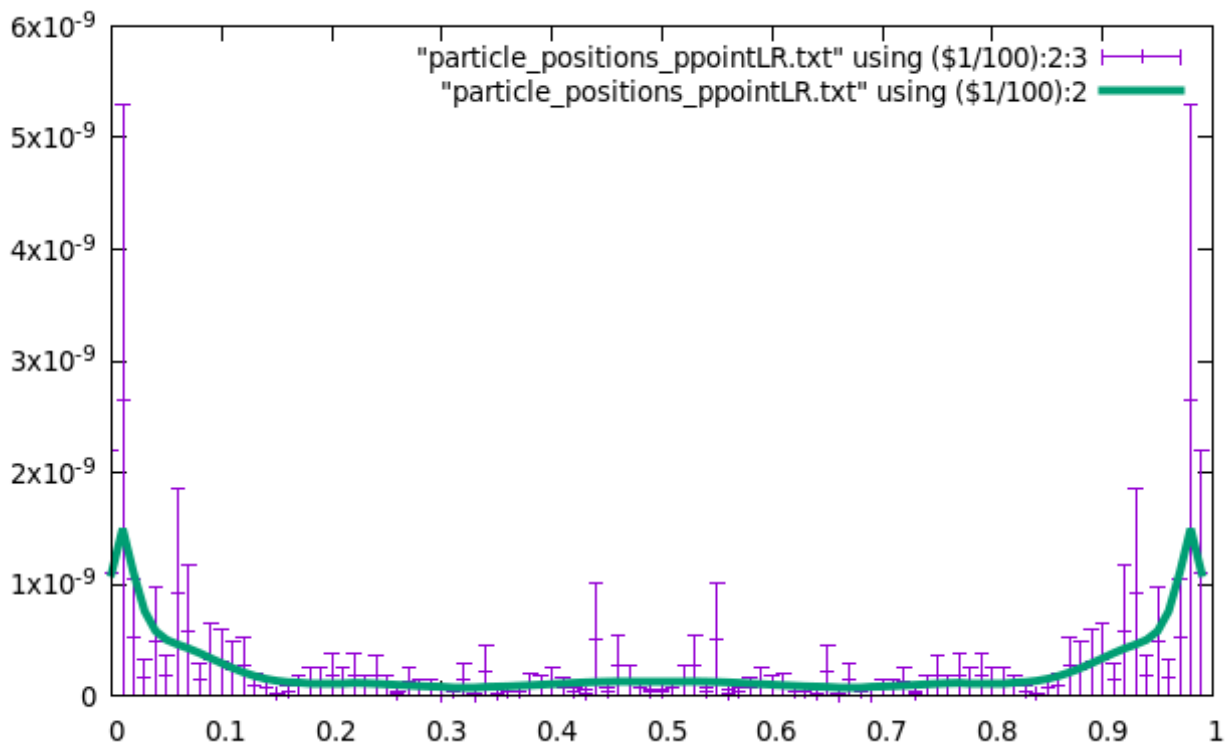


Figure 12 — the rotation rate according to the height at the wall for the « low » flow and an aspect ratio $\alpha=1$
 © Bouilliez, Gilbert, Lepêtre

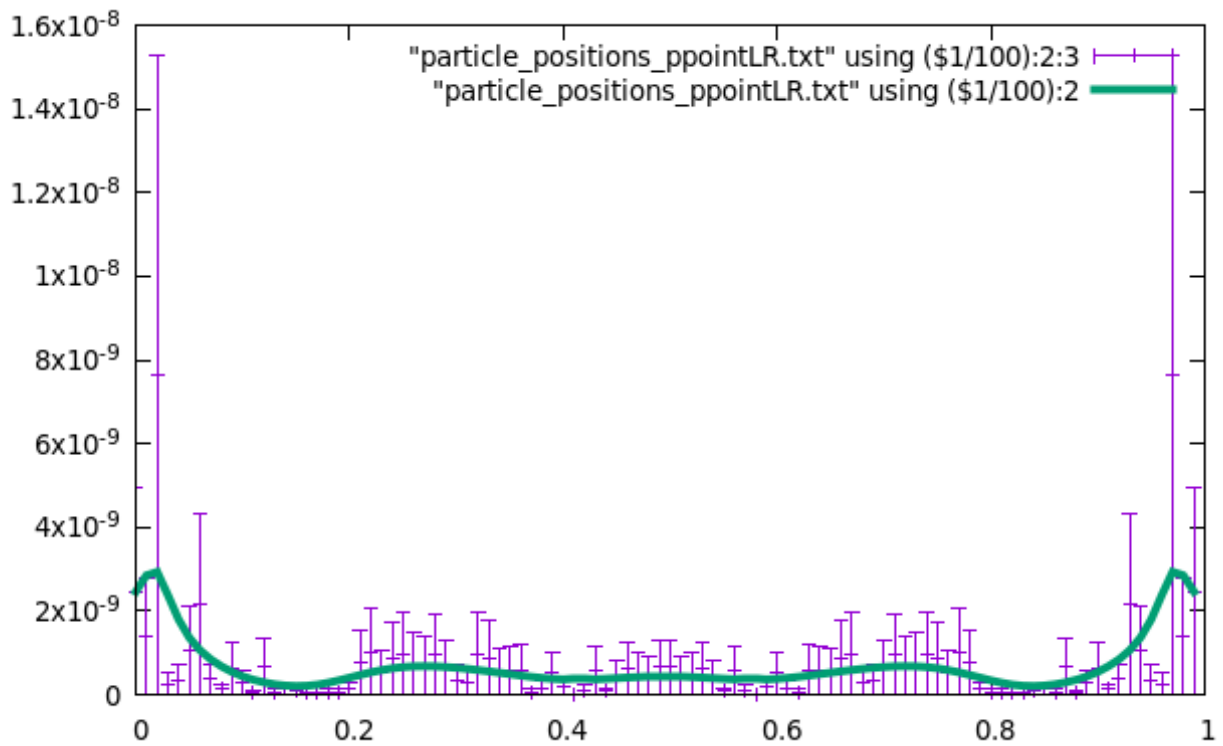


Figure 13 — the rotation rate according to the height at the wall for the « low » flow and an aspect ratio $\alpha=2.8$ © Bouilliez, Gilbert, Lepêtre

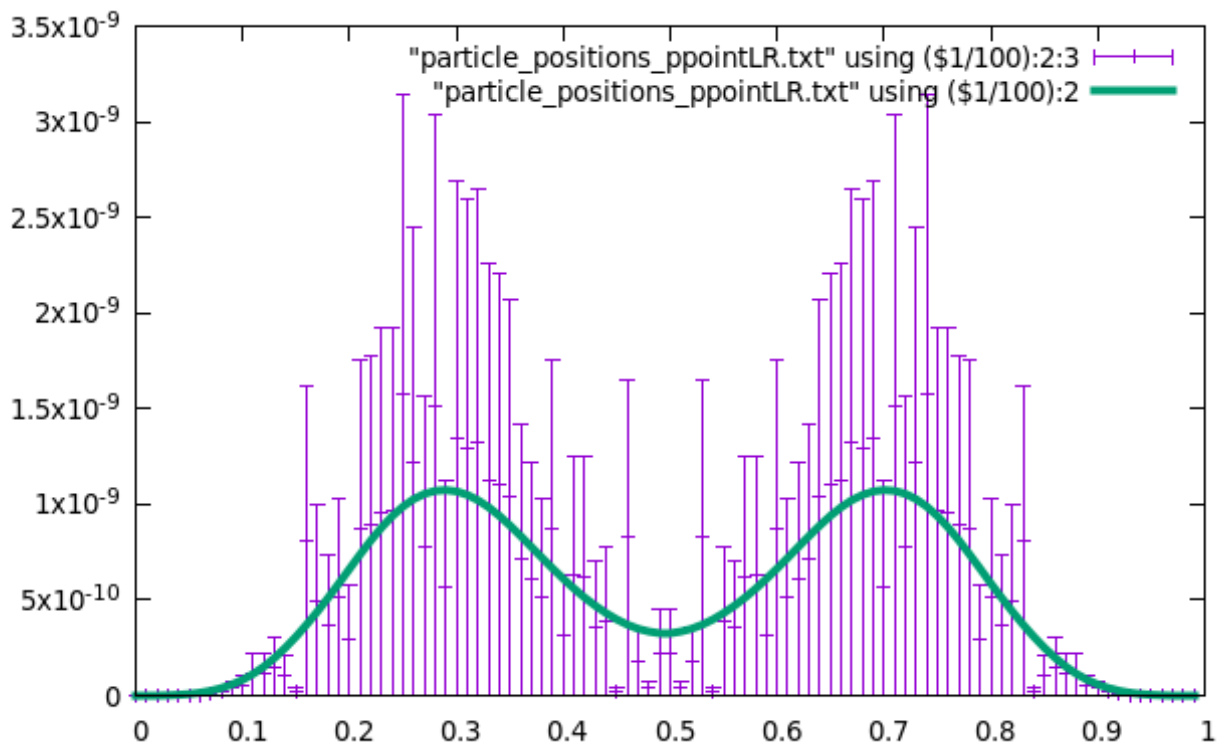


Figure 14 — the rotation rate according to the height at the wall for the « low » flow and an aspect ratio $\alpha=100$ © Bouilliez, Gilbert, Lepêtre

To study this rotation rate, we started by simulating a flow in which the placed particles have an aspect ratio equal to 1, that is to say when the particles are spheres. Then, we simulated a flow in which the particles have an aspect ratio of 2.8 and to finish, we simulated a flow in which the particles have an aspect ratio of 100.

By studying these three graphs, we notice that for $\alpha=1$, we observe large peaks at the wall whereas for $\alpha=100$, we notice that these peaks at the wall have totally disappeared. Thus, for the low Rayleigh flow, we can say that when we increase the anisotropy of the particles of the flow, we reduce the rotation rate to the wall. This implies that, as we already said for M , the spherical particles do not have preferential orientations.

b. Flow « high »

In a first step, we will study the variation of the rotation rate for the « high » flow, that is the least stable turbulent flow.

As for the « low » flow, we used particles of different aspect ratios to study the rotation rate. Therefore, we first simulated a flow in which we placed particles with an aspect ratio equal to 1, that is to say that they are spherical particles. Then, we simulated a flow in which the particles have an aspect ratio of 2.8 and finally, we simulated a flow in which the particles have an aspect ratio of 100.

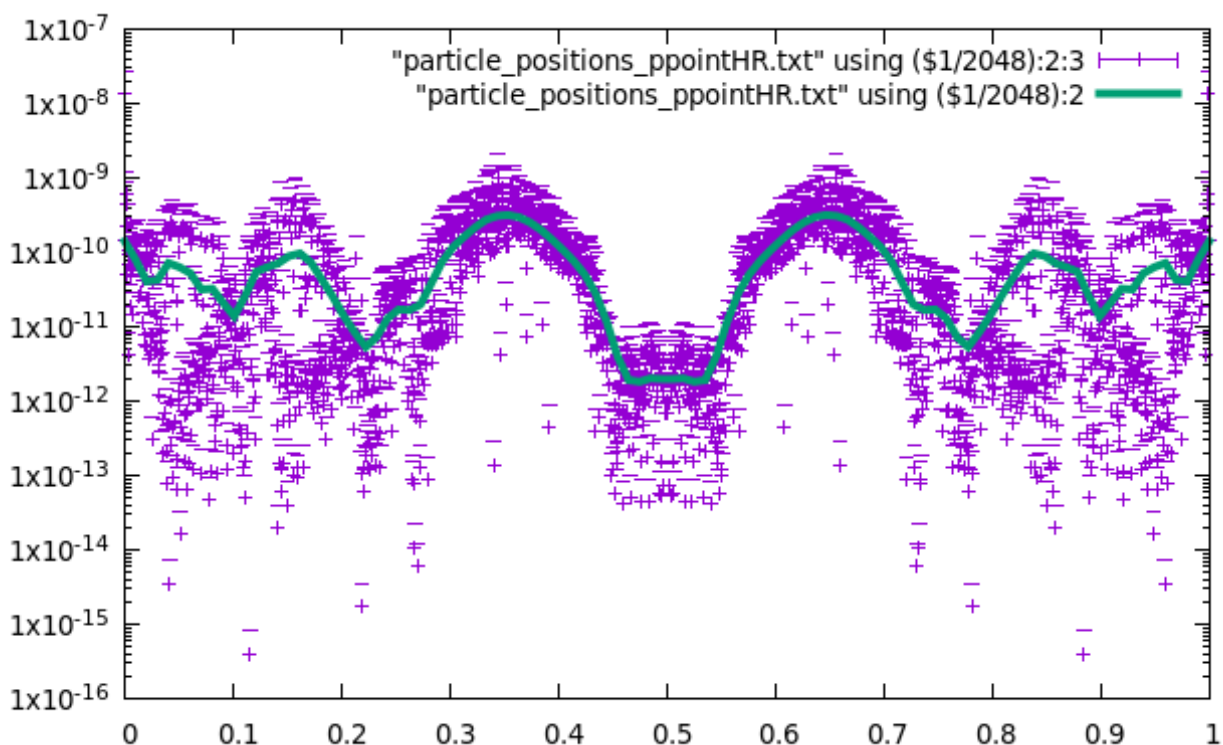


Figure 15 — the rotation rate according to the height at the wall for the « high » flow and an aspect ratio $\alpha=1$ © Bouilliez, Gilbert, Lepêtre

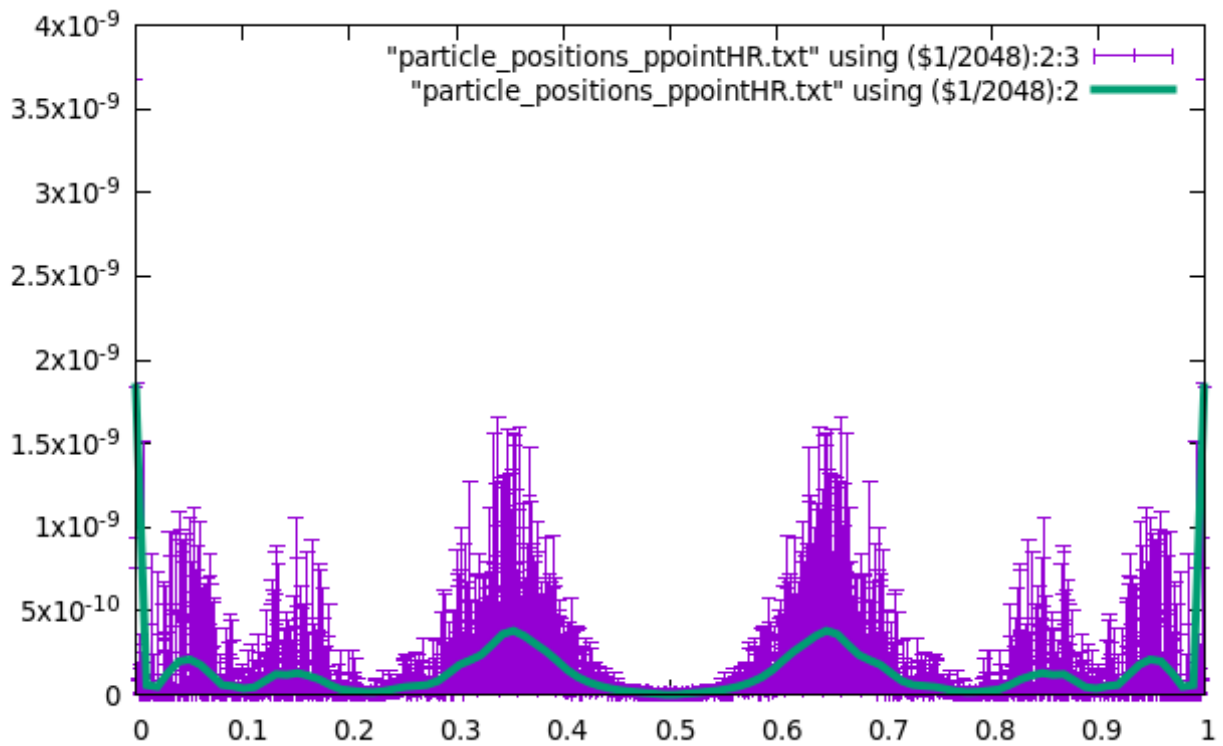


Figure 16 — the rotation rate according to the height at the wall for the « high » flow and an aspect ratio $\alpha=2.8$ © Bouilliez, Gilbert, Lepêtre

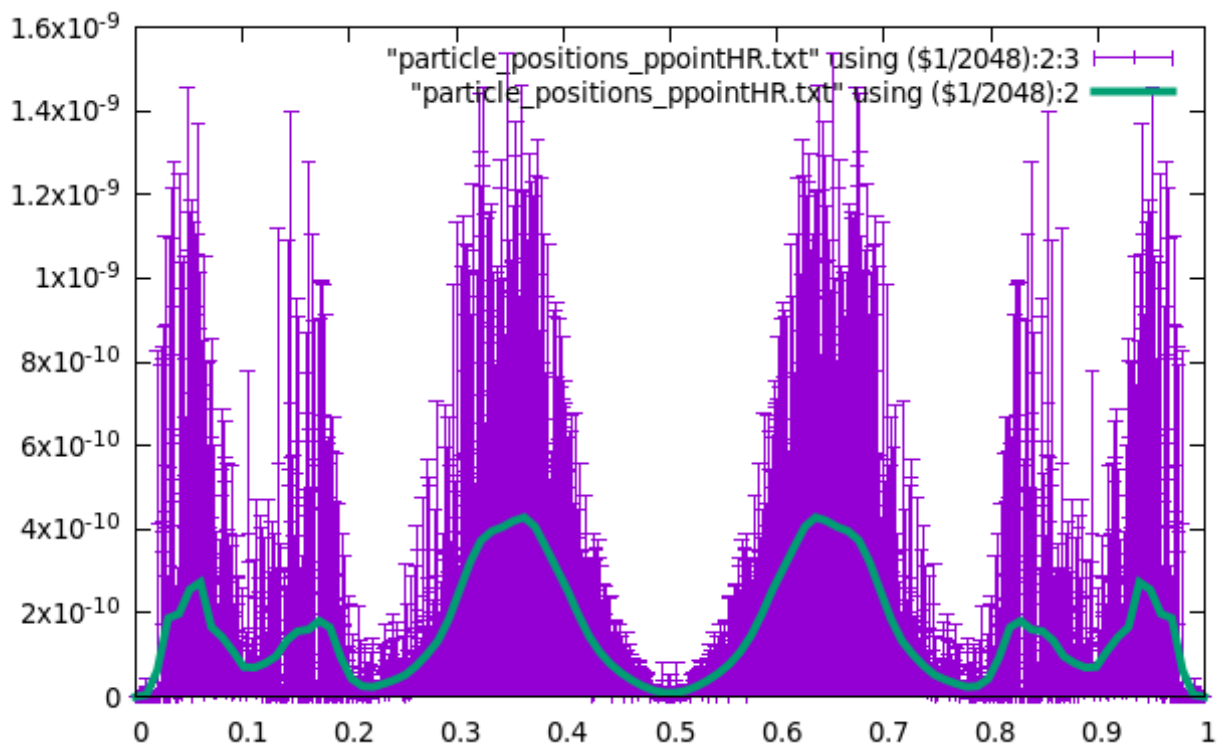


Figure 17 — the rotation rate according to the height at the wall for the « high » flow and an aspect ratio $\alpha=100$ © Bouilliez, Gilbert, Lepêtre

First, we can compare the graph « low » and « high » for an aspect ratio $\alpha=1$. We notice that the peaks at the wall decrease when the Rayleigh number increases.

Then, when we look at the graph « high » for $\alpha=100$, we notice that the rotation rate curve goes to 0, and this region is very small. This implies that the rotation speed is extremely low near the wall, which seems logical because the particles are aligned horizontally according to the study of M carried out previously. We could then look at this phenomenon and ask why the rotation speed is much lower near the wall.

Near the wall, there is what is called a boundary layer. At this point, the flow is much more dominated by the presence of viscosity than by turbulence. This boundary layer varies depending on the distance to the wall.

Near the wall, the velocity gradient has only one component:

$$\nabla U = \begin{pmatrix} 0 & \frac{\partial u_x}{\partial y} \\ 0 & 0 \end{pmatrix}$$

This gradient, when it is used in the Jeffery's equation, and assuming that $\frac{du_x}{dy}$ is

constant, provides a solution. The equation of Jeffery makes it possible to affirm that the velocity of a particle, if it is a sphere, is constant in time. However, for an elongated particle, we will be able to observe a higher rotational speed for a particle in an oblique position than for a particle in a horizontal position. In fact, the rotational speed of a particle in an oblique position will be higher and this will be due to the differences of velocities that the particle suffers at its different points. For an horizontally particle, the rotational speed of the particle is minimal because the particle is positioned for an $y=\text{constant}$ and thus the velocity of the flow, is also constant. Here is a diagram (figure n°18) for visualizing the reason for the difference of rotation speed between a particle positioned at the oblique and a particle positioned vertically.

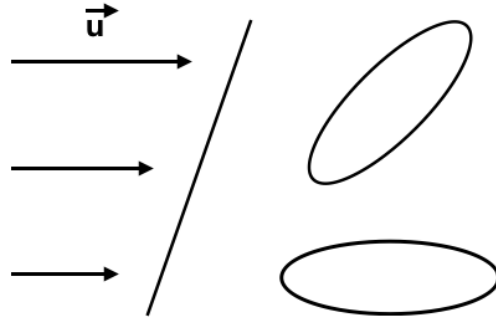


Figure 18 — influence of the alignment of particles on the rotation speed © Bouilliez, Gilbert, Lepêtre

with \vec{u} the velocity field of the flow

This explains why, near the wall, the elongated fibers are horizontal whereas the spheres have no preferential alignment and that the orientation of the spheres is distributed randomly.

Thus, we can say that the alignment of the particles is not related to the fact that there is an interaction between the particles and the walls because the particles do not see the wall but they feel its presence through the flow that is dominated by one direction.

The spherical particles represent a special case and, although in our project we mainly had to study the anisotropic particles, we also wanted to understand the evolution of spherical particles in a turbulent flow, in order to be able to compare this type of particles with the elongated particles. Previously, we demonstrated that in the two-dimensional case, $\dot{p}^2 = \dot{\theta}^2$. Now, thanks to the equation of Jeffery, we know that $\dot{\theta} = \frac{1}{2}\omega - \lambda [S_{11} \sin(2\theta) - S_{12} \cos(2\theta)]$. However, in the case of a spherical particle,

the equation of Jeffery is greatly simplified and becomes: $\dot{\theta} = \frac{1}{2}\omega$. So, like $\dot{p}^2 = \dot{\theta}^2$, we

have $\dot{p}^2 = \frac{1}{4}\omega^2$. Therefore, we can say that a sphere-shaped particle will always have a

rotational speed equal to half of the vorticity. Therefore, we can say that the rotation speed of this type of particle is proportional to the intensity of the vorticity, which implies that the speed of rotation is proportional to the turbulence.

We were able to use the data obtained, but we noticed that much more data would have been needed to obtain solid conclusions. Thus, it would be necessary to have much longer simulations.

To conclude, the spherical particles have speed of rotation that is proportional to the vorticity, and it's constant in the case of plane shear flow, as it happens close to the walls in the system we have here studied. Thus, they do not have a preferential orientation, regardless of where they are in the flow. Therefore this type of particle has no preferential alignment because its orientation varies randomly and this is due to its rotational speed.

Concerning the anisotropic particles, we notice that they have a preferential orientation, especially near the walls where they are horizontally aligned because, as we saw during the study of the rotation rate, near the wall, the rotation speed of the particles is minimal when they are parallel to the walls. However, we have noted that the intensity of the turbulence has a great influence on the preferential orientation of the particles. In fact, when the turbulence is rather weak, that is to say when the Rayleigh number is small, we notice that the particles located in the middle of the flow seem to align preferentially according to the vertical whereas when the turbulence becomes high, the Rayleigh number is very large, we no longer observe preferential alignment for the particles in the middle of the flow, their orientation now varies randomly. Thus, we can say that it is difficult to predict the orientation of a particle within the vortices of a convective flow. Moreover, when the intensity of the turbulence increases, we notice that the zone where the anisotropic particles align horizontally near the walls decreases very widely. Generally, we can say that when the turbulence increases, the prediction of particle orientation becomes more and more difficult, whether for particles in the middle of the flow or those located at the walls.

Conclusion

In order to study the dynamics of a particle under the effect of a turbulent flow, we asked ourselves the following question: « How does the orientation and the speed of rotation of a particle vary in a turbulent flow? ».

To better understand this project, we became interested in the applications of the "everyday" life, and realized that understanding the evolution of particles in a turbulent flow could allow a considerable advance. Indeed, thanks to this, one can predict the dispersion of the smoke of a volcano for example, or any other problem related to the dynamics of a particle. However, by looking at the equations allowing to understand the evolution of particles in a turbulent flow, we noticed that these, are very difficult to solve because of their non-linearity. This is why, to simplify these equations, we have placed ourselves in the two-dimensional case.

By performing numerical simulations, we realized that for a low turbulent flow, that is to say with a low Rayleigh number, the particles seemed to align horizontally at the walls, while having a minimal rotation velocity. However, in the center of the flow, the particles seemed to align vertically. With regard to the very turbulent flow, with the high Rayleigh number, we noticed that the particles remained aligned at the walls. Moreover, we have seen that the particles in the center of the flow, that is to say in the vortices, had no preferential orientation.

Therefore, we might ask what happens in the center of a turbulent flow. Can we even predict what is happening there? We would need a lot of data to be able to imagine providing an answer to this question. Indeed, the more the data we will have, the more the statistics will converge and we can then be able to predict what happens at the center of a turbulent flow.

All the same, we notice that the alignment of the particles is related to the structure of the flow in which they evolve, that is to say if the flow is more or less turbulent. We could then use these particles as a flow visualization tool to learn more about the flow.

Bibliography

THESES

BYRON, Margaret. *The rotation and translation of non-spherical particles in homogeneous isotropic turbulence*. Doctoral thesis: Engineering - Civil and Environmental. Berkeley: University of California, 2015, 145 p.

VINCENZI, Dario. *Dynamique lagrangienne en turbulence et turbulence élastique*. Ability to conduct researches. University of Côte d'Azur, 2018, 246 p.

PARSA MOGHADDAM, Shima. *Rotation dynamics of rod particles in fluid flows*. Doctoral thesis: physics. Middletown: Wesleyan University, 2013, 97 p.

GIBERT, Mathieu. *Convection thermique turbulente: Panaches et fluctuations*. Doctoral thesis: physics. University of Lyon, 2007, 182 p.

ARTICLES

OLSON James A. and KEREKES Richard J. The motion of fibres in turbulent flow. *Journal of Fluid Mechanics*. 1998, Vol 377, pp. 47-64.

PARSA S., GUASTOS J.S., KISHORE M., OUELLETTE N.T., GOLLUB J.P. Rotation and alignment of rods in two-dimensional chaotic flow. *G.A.Voth Physics of Fluids 23, American Institute of Physics*. 2011, Vol 23.

PARSA S., CALZAVARINI E., TOSCHI F. and VOTH G. A. Rotation Rate of Rods in Turbulent Fluid Flow. *Physical Review Letters*. September 28 2012, Vol 109.

GUPTA A., VINCENZI D. and PANDIT R. Elliptical tracers in two-dimensional, homogeneous, isotropic fluid turbulence: The statistics of alignment, rotation, and nematic order. *Physical Review Letters*. February 19 2014, Vol 89.

VOTH G. A. and SOLDATI A. Anisotropic particles in turbulence. *Annual review of fluid mechanics*. Janvier 2017, vol. 49, pp. 249-276.

<https://www.annualreviews.org/doi/abs/10.1146/annurev-fluid-010816-060135>

Annex

```
h5_field_and_particles_plot_2d.py
# This script visualize the temperature field, the streamlines and the
particles.

#!/usr/local/bin/python
import h5py
import numpy as np
import sys
import math
import matplotlib
import matplotlib.pyplot as plt

f = h5py.File('Data/RUN_highRa1/field_10000.h5', 'r')
#f = h5py.File('../Data/RUN_highRa1/field_5000.h5', 'r')
#f = h5py.File('/Users/enrico/field_135000.h5', 'r')
t=np.array(f['euler']['temperature'])
vx=np.array(f['euler']['velocity_x'])
vy=np.array(f['euler']['velocity_y'])
x=np.array(f['euler']['position_x'])
y=np.array(f['euler']['position_y'])

NZ = t.shape[0]
NY = t.shape[1]
NX = t.shape[2]
print("NZ= "+str(NZ))
print("NY= "+str(NY))
print("NX= "+str(NX))
tslice=t[0,:,:]
strivev=2
strivey=2
vxslice=vx[0,0:NY:strivev,0:NX:strivev]
vyslice=vy[0,0:NY:strivev,0:NX:strivev]
xslice=x[0,0:NY:strivev,0:NX:strivev]
yslice=y[0,0:NY:strivev,0:NX:strivev]
speed = np.sqrt(vxslice*vxslice + vyslice*vyslice)
lw = 1.5*speed / speed.max()

fig, ax = plt.subplots(subplot_kw={'aspect': 'equal'})
ax.set_xlim(0, NX)
ax.set_ylim(0, NY)
ax.axis((0,NX,0,NY))
ax.imshow(tslice, cmap='seismic') #for color map https://matplotlib.org/
tutorials/colors/colormaps.html
ax.streamplot(xslice,yslice,vxslice,vyslice,
density=2,linewidth=lw,color="gray",arrowsize=0.5)

p = h5py.File('Data/RUN_highRa1/particle_10000.h5', 'r')
#p = h5py.File('../Data/RUN_highRa1/particle_5000.h5', 'r')
#p = h5py.File('/Users/enrico/particle_135000.h5', 'r')

xpart=np.array(p['lagrange']['x'])
ypart=np.array(p['lagrange']['y'])
pxpart=np.array(p['lagrange']['px'])
pypart=np.array(p['lagrange']['py'])
ar=np.array(p['lagrange']['aspect_ratio'])

npart = ar.shape[0]
ar_types=np.asarray(list(set(ar)))
ar_types=np.sort(ar_types)
n_ar_types=len(ar_types)
print("ar_types = "+str(ar_types))
print("n_ar_types = "+str(n_ar_types))

# Now I add the ellipses
from matplotlib.patches import Ellipse

ells=[]
for i in range(npart):
    if ar[i]==ar_types[0]:
        ells.append(Ellipse(xy=(xpart[i], ypart[i]),
width=1.5, height=ar[i]/40.,
angle=np.arcsin(pxpart[i])/np.pi*180.,
zorder=10))

for e in ells:
    ax.add_artist(e)
    e.set_clip_box(ax.bbox)
    e.set_facecolor("black")

plt.savefig('visual10000.png', dpi=256)
plt.show()
```

Annex 1 — computer program, in Python, allowing to visualize the flow © Bouilliez, Gilbert, Lepêtre

```

programmeMHR.py
#!/usr/local/bin/python
from __future__ import print_function
import h5py
import numpy as np

NY=2048
px_square = np.zeros(NY)
count = np.zeros(NY)

# set the name of the file to be read
for i in range(5000,20000,5000):
# open the file
    fin = h5py.File("Data/RUN_highRa1/particle_%d.h5" % i,'r')
# open the dataset in the file
    group = fin['lagrange']
# get the labels of the available subdataset
    labels = group.keys()
    print("The available data in the file are the following: "+str(labels))

# transfer the data to numpy arrays
    name=np.array( group['name'])
    y=np.array( group['y'])
    px=np.array( group['px'])
    ar=np.array( group['aspect_ratio'])
    npart = name.shape[0]

    for j in range(0,npart):
        n=int(y[j])
        if 2.7<ar[j]<2.8:
            px_square[n] += px[j]*px[j]
            count[n] = count[n] + 1

# set the output filename
    foutname = 'particle_positions_MHR.txt'
    fout = open(foutname,'w')

#write the data on the file
    for j in range(0,NY):
        print(j,(1./2.)*((2*px_square[j]/count[j])+(2*px_square[NY-1-j]/
count[NY-1-j])-2), abs((1. /2.)*((2*px_square[j]/count[j])-(2*px_square[NY-1-j]/
count[NY-1-j]))), file=fout)

# close all the open files
    fout.close()
    fin.close()

    print(ar)

```

Annex 2 — computer program, in Python, allowing to plot the curves of the parameter M according to the height at the wall © Bouilliez, Gilbert, Lepêtre

```

programme_ppointHR.py
#!/usr/local/bin/python
from __future__ import print_function
import h5py
import numpy as np

NY=2048
dt_p_square = np.zeros(NY)
count = np.zeros(NY)

# set the name of the file to be read
for i in range(5000,20000,5000):
# open the file
    fin = h5py.File("Data/RUN_highRa1/particle_%d.h5" % i,'r')
# open the dataset in the file
    group = fin['lagrange']
# get the labels of the available subdataset
    labels = group.keys()
    print("The available data in the file are the following: "+str(labels))

# transfer the data to numpy arrays
    name=np.array( group['name'])
    y=np.array( group['y'])
    dt_px=np.array( group['dt_px'])
    dt_py=np.array( group['dt_py'])
    ar=np.array( group['aspect_ratio'])
    npart = name.shape[0]

    for j in range(0,npart):
        n=int(y[j])
        if 2.7<ar[j]<2.8:
            count[n] = count[n] + 1
            dt_p_square[n] = dt_px[j]*dt_px[j] + dt_py[j]*dt_py[j]

# set the output filename
    foutname = 'particle_positions_ppointHR.txt'
    fout = open(foutname,'w')

#write the data on the file
    for j in range(0,NY):
        print(j,abs((1./2.)*((dt_p_square[j]/count[j])-(dt_p_square[NY-1-j]/count[NY-1-j]))), abs((1./2.)*((dt_p_square[j]/count[j])-(dt_p_square[NY-1-j]/count[NY-1-j]))),file=fout)

# close all the open files
    fout.close()
    fin.close()

```

Annex 3 — computer program, in Python, allowing to plot the curves of the rotation rate according to the height at the wall © Bouilliez, Gilbert, Lepêtre